RSC Advances

ROYAL SOCIETY OF CHEMISTRY

www.rsc.org/advances

Graphical Abstract

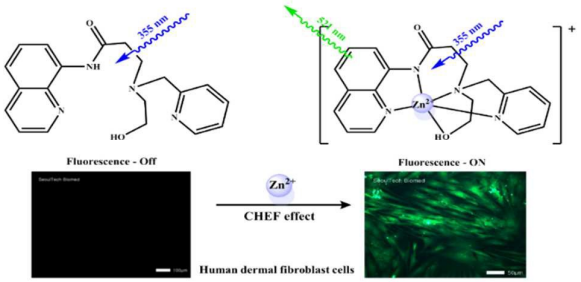

A new quinolone-based chemosensor was synthesized and successfully applied to quantify and image Zn^{2+} in water samples and living cells.

A highly selective CHEF-type chemosensor for monitoring Zn^{2+} in aqueous solution and living cells

Jae Jun Lee,[a] Seul Ah Lee,[a] Hyun Kim,[a] LeTuyen Nguyen,[b] Insup Noh,[b] Cheal Kim[a]*

[a]*Department of Fine Chemistry and Department of Interdisciplinary Bio IT Materials, Seoul National University of Science and Technology, Seoul 139-743, Republic of Korea. Fax: +82-2-973-9149; Tel: +82-2-970-6693; E-mail: chealkim@seoultech.ac.kr*
[b]*Department of Chemical and Biomolecular Engineering, and Convergence Program of Biomedical Engineering and Biomaterials, Seoul National University of Science & Technology, Seoul 139-743, Republic of Korea.*

Abstract

A new simple quinolone-based chemosensor **1** was synthesized for Zn^{2+}. **1** exhibited the selective fluorescence enhancement in the presence of Zn^{2+} with a 1:1 stoichiometry in aqueous solution, which was reversible with the addition of ethylenediaminetetraacetic acid (EDTA). The detection limit (0.019 μM) of **1** for Zn^{2+} is far lower than World Health Organization guideline (76 μM) in drinking water. **1** was successfully applied to quantify and image Zn^{2+} in water samples and living cells. The sensing mechanism of Zn^{2+} by **1** via the chelation-enhanced fluorescence (CHEF) effect was supported by theoretical calculations. Therefore, **1** could be used in a practical system for monitoring Zn^{2+} in aqueous solution.

Keywords: fluorescent chemosensor, zinc ion, CHEF effect, cell imaging, theoretical calculations

Introduction

Zinc ion is one of the most abundant metal ions present in living organism, owing to its rich coordination chemistry. [1-4] Although most of the Zn^{2+} ions in a cell are tightly bound to metalloproteins, free forms are also found throughout the cell. In the brain, 5-20% of the total Zn^{2+} is stored in presynaptic vesicles, and the highest intracellular free Zn^{2+} is found in the hippocampus.[5-6] Zn^{2+} modulates brain excitability and plays a key role in synaptic plasticity.[7-8] On the other hand, the deficiency of zinc causes unbalanced metabolism, which in turn can induce retarded growth in children, brain disorders and high blood cholesterol, and also be implicated in various neurodegenerative disorders such as Alzheimer's disease, epilepsy, ischemic stroke, and infantile diarrhea.[9-15] In addition, an excess of zinc in the environment may reduce the soil microbial activity which results in phytotoxic effect.[16-21] Therefore, selective detection and quantification for zinc ion is very important object of increasing investigation.[22-24]

A variety of traditional methods (e.g. inductively coupled plasma atomic emission spectrometry, atomic absorption spectroscopy, and electrochemical methods) have been developed for analyses of zinc in environmental samples and for diagnosis of their deficiencies in body tissue.[25-28] However, these methods require sophisticated instrumentations, tedious sample preparation procedures, and trained operators. By contrast, chemosensors are highly estimable means for the selective recognition of chemicals and biological species in environmental chemistry and biology.[29] The design of chemosensors with high selectivity and sensitivity for zinc, is currently of great importance as they allow nondestructive and prompt detection of metal ions by simple fluorescence enhancement (turn-on) responses.[22-24] Especially, the development of chemosensors that can discriminate Zn^{2+} from Cd^{2+} is still a huge challenge as they are in the same group of the Periodic table and have similar properties.[30-33] Thus, low cost and easily-prepared Zn^{2+} fluorescence chemsensors are needed for convenience.[34-41]

In view of this requirement and as part of our research effort devoted to zinc ion recognition, we have considered the combination of a quinoline moiety and a 2-(ethyl(pyridin-2-yl)amino)ethan-1-ol (**2**, see Scheme 1) unit.[22,42-45] In particular, we expected that the ethanol group would make water-solubility of **1** increase. Additionally, we theoretically expected that fluorescence enhancement was originated from the stabilization of quinoline group. Finally, we synthesized a new type of water-soluble chemosensor **1** (Scheme 1) by combining the

quinolone group with **2**, and tested its sensing properties towards various metal ions.

Herein, we report a new chemosensor **1**, composed of the quinoline and 2-(ethyl(pyridin-2-yl)amino)ethan-1-ol. **1** showed an intense fluorescence enhancement in the presence of zinc ions in aqueous solution, could distinguish Zn^{2+} from Cd^{2+}, and sensed quantitatively Zn^{2+} in living cells for practical application. Additionally, the experimental data and the sensing mechanism were supported by theoretical calculations.

Experimental section

Materials and instrumentation

All the solvents and reagents (analytical grade and spectroscopic grade) were obtained commercially and used as received. NMR spectra were recorded on a Varian 400 spectrometer. Chemical shifts (δ) were reported in ppm, relative to tetramethylsilane $Si(CH_3)_4$. Absorption spectra were recorded at 25℃ using a Perkin Elmer model Lambda 2S UV/Vis spectrometer. The emission spectra were recorded on a Perkin-Elmer LS45 fluorescence spectrometer. Electrospray ionization mass spectra (ESI-MS) were collected on a Thermo Finnigan (San Jose, CA, USA) LCQTM Advantage MAX quadrupole ion trap instrument. Elemental analysis for carbon, nitrogen, and hydrogen was carried out by using a Flash EA 1112 elemental analyzer (thermo) in Organic Chemistry Research Center of Sogang University, Korea. 3-Chloro-N-(quinolin-8-yl)propanamide was obtained from the previous study.[34]

Synthesis of sensor 1

2-Aminoethanol (0.97 mL, 10 mmol) and picolinaldehyde (0.61 mL, 10 mmol) were dissolved in ethanol (15 mL) and stirred for 3 h. Then, $NaBH_4$ (0.38 g, 10.2 mmol) was added, and the reaction solution was cooled in an ice bath. It was stirred for 2 h and the solvent was removed under reduced pressure to obtain colorless oil (**2**) (Scheme 1). Yield of **2** was 1.05 g (69 %). The colorless oily residue (**2**) was dissolved in methylene chloride and then the solution was washed twice with water. Organic layer was dried over anhydrous Na_2SO_4 and the solvent was evaporated under vacuo. The resultant product **2** (0.30 g, 2 mmol), 3-chloro-N-(quinolin-8-yl)propanamide (0.49 g, 2.2 mmol) and triethylamine (TEA, 0.28 mL, 2 mmol) were dissolved in tetrahydrofuran (THF, 30 mL), stirred and refluxed for 1 d. The mixture was cooled down to room temperature and the solvent was removed under reduced pressure to obtain brown oil, which was purified by silica gel column chromatography (9 : 1 v/v $CHCl_3$-CH_3OH).

Yield: 0.49 g (73 %). ^{1}H NMR (400 MHz, DMSO-d_6, 25 °C): δ = 10.88 (s, 1H), 8.86 (d, *J* = 8.9 Hz, 1H), 8.65 (d, *J* = 8.7 Hz, 1H), 8.43 (d, *J* = 8.4 Hz, 1H), 8.40 (d, *J* = 8.4 Hz, 1H), 7.66-7.51 (m, 2H), 7.57 (d, *J* = 7.6 Hz, 1H), 7.53 (m, 2H), 7.49 (t, *J* = 7.1 Hz, 1H), 4.45 (t, *J* = 4.4 Hz, 1H), 3.89 (s, 2H), 3.58 (t, *J* = 3.6 Hz, 2H), 2.93 (t, *J* = 3.0 Hz, 2H), 2.49 (m, *J* = 2.9 Hz, 4H) ppm. ^{13}C NMR (100 MHz, DMSO-d_6, 25 ℃): δ = 171.7 (1C), 156.7 (2C), 147.1 (2C), 139.9 (1C), 138.8 (1C), 129.8 (1C), 129.0 (1C), 127.7 (1C), 127.5 (1C), 126.0 (2C), 124.8 (1C), 122.8 (2C), 121.8 (1C), 121.5 (1C), 110.2 (1C), 21.8 (1C) ppm. LRMS (ESI): m/z calcd for $C_{20}H_{22}N_4O_2$-H^++Zn^{2+}: 413.095; found 413.267. Elemental analysis calcd (%) for $C_{20}H_{22}N_4O_2$: C, 68.55; H, 6.33; N, 15.99; found: C, 68.65; H, 5.95; N, 15.75.

Fluorescence titration of 1 with Zn^{2+}

Sensor **1** (0.5 mg, 0.0015 mmol) was dissolved in MeOH (0.5 mL) and 10 μL of the sensor **1** (3 mM) were diluted to 2.990 mL bis-tris buffer solution (10 mM, pH 7.0) to make the final concentration of 10 μM. $Zn(NO_3)_2$ (0.01 mmol) was dissolved in bis-tris buffer solution (1 mL) and 0.3-4.8 μL of the Zn^{2+} solution (10 mM) were added to the sensor **1** solution (10 μM, 3 mL) prepared above. After mixing them for a few seconds, fluorescence spectra were obtained at room temperature. Identical results were also obtained in pure water.

UV-vis titration of 1 with Zn^{2+}

Sensor **1** (0.5 mg, 0.0015 mmol) was dissolved in MeOH (0.5 mL) and 10 μL of the sensor **1** (3 mM) were diluted to 2.990 mL bis-tris buffer solution (10 mM, pH 7.0) to make the final concentration of 10 μM. $Zn(NO_3)_2$ (0.01 mmol) was dissolved in bis-tris buffer solution (1 mL) and 0.3-4.8 μL of the Zn^{2+} solution (10 mM) were transferred to separate sensor solutions (10 μM, 3 mL). After mixing them for a few seconds, UV-vis spectra were taken at room temperature.

^{1}H NMR titration of 1 with Zn^{2+}

Five NMR tubes of **1** (0.7 mg, 0.002 mmol) dissolved in in D_2O/CD_3OD (9:1, v/v) were prepared, and five different equivalents (0, 0.3, 0.5, 1 and 1.5 equiv) of zinc nitrate dissolved in D_2O (0.5 mL) were added separately to the solutions of **1**. After shaking them for a few seconds, the ^{1}H NMR spectra were taken.

Methods of cell test of 1 with Zn^{2+}

Human dermal fibroblast cells in low passage were cultured in FGM-2 medium (Lonza, Switzerland) supplemented with 10% fetal bovine serum, 1% penicillin/streptomycin in the in vitro incubator with 5% CO_2 at 37 ℃. Cells were seeded onto a 8 well plate (SPL Lifesciences, Korea) at a density of 2×10^5 cells per well and then incubated at 37 ℃ for 4 h after addition of various concentrations (0-100 μM) of $Zn(NO_3)_2$ dissolved in MeOH. After washing with phosphate buffered saline (PBS) two times to remove the remaining $Zn(NO_3)_2$, the cells were incubated with **1** (20 μM) dissolved in MeOH at room temperature for 1 h. The cells were observed using a microscope (Olympus, Japan). The fluorescent images of the cells were obtained using a fluorescence microscope (Leica DMLB, Germany) at the excitation wavelength of 425 nm. The relative fluorescence intensity of fluorescence microscopy images was evaluated by Icy software.[46] The four cell-body regions in visible field (green light source) were randomly selected as the region of interest to determine the average fluorescence intensity.

Determination of Zn^{2+} in water samples

Fluorescence spectral measurement of water samples containing Zn^{2+} were carried by adding 20 μL of 3 mmol/L stock solution of **1** and 0.60 mL of 50 mmol/L bis-tris buffer stock solution to 2.38 mL sample solutions. After well mixed, the solutions were allowed to stand at 25 ˚C for 2 min before the test.

Method for theoretical calculations of 1 and 1-Zn^{2+} complex

All theoretical calculations were performed by using the Gaussian 03 suite.[46] The singlet ground states (S_0) of **1** and **1**-Zn^{2+} complex were optimized by DFT methods with Becke's three parametrized Lee-Yang-Parr (B3LYP) exchange functional[47-48] with 6-31G** basis set[49-50]. In vibrational frequency calculations, there was no imaginary frequency for **1** and **1**-Zn^{2+} complex, suggesting that the optimized **1** and **1**-Zn^{2+} complex represented local minima.

Results and discussion

Synthesis of 1

The compound **2** (2-((pyridin-2-yl)methylamino)ethanol) was synthesized by condensing

2-aminoethanol and picolinaldehyde in ethanol (Scheme 1). Subsequently, the substitution reaction of **2** to 3-chloro-N-(quinolin-8-yl)propanamide afforded **1**, which was characterized by ^{1}H NMR, ^{13}C NMR, ESI-mass, spectrometry and elemental analysis.

Fluorescence and absorption spectroscopic studies of 1 toward Zn^{2+}

The fluorescent behavior of **1** toward various metal ions was studied in bis-tris buffer solution (10 mM, pH 7.0). When excited at 355 nm, **1** exhibited a weak fluorescence emission (λ_{max} = 521 nm) compared to that (37-folds) in the presence of Zn^{2+} (Fig. 1). In contrast, upon addition of other metal ions such as Na^{+}, K^{+}, Mg^{2+}, Ca^{2+}, Al^{3+}, Ga^{3+}, Cr^{3+}, Mn^{2+}, Fe^{2+}, Fe^{3+}, Co^{2+}, Ni^{2+}, Cu^{2+}, Zn^{2+}, Ga^{3+} and Pb^{2+}, no increase in intensity was observed. These results indicated that sensor **1** could be used as a fluorescence chemosensor for Zn^{2+}. The selective fluorescence enhancement response to Zn^{2+} might be due to the effective coordination of Zn^{2+} with **1** over other metal ions, which might be attributed to the operation of CHEF (chelation enhanced fluorescence) mechanism.[31,51]

To further investigate the chemosensing properties of **1**, fluorescence titration of the sensor **1** with Zn^{2+} ion was performed. As shown in Fig. 2, the emission intensity of **1** at 521 nm steadily increased until the amount of Zn^{2+} reached 1.2 equiv. The photophysical properties of **1** were also examined using UV-vis spectrometry. UV-vis absorption spectrum of **1** showed two absorption bands at 237 and 302 nm (Fig. S1). Upon the addition of Zn^{2+} ions to a solution of **1**, the two bands have red-shifted to 253 and 351 nm, respectively. Meanwhile, three clear isosbestic points were observed at 243, 280 and 325 nm, suggesting that only one product was produced from the binding of **1** with Zn^{2+}.

The Job plot[52] showed a 1:1 complexation stoichiometry between **1** and Zn^{2+} (Fig. S2), which was further confirmed by ESI-mass spectrometry analysis (Fig. 3). The positive-ion mass spectrum of **1** upon addition of 1 equiv of Zn^{2+} showed the formation of the **1**-H^{+}+Zn^{2+} [m/z: 413.267; calcd, 413.095]. Based on pK_a values (11.9 vs 15.8) of the acetamide and ethanol moieties reported in the literatures[53], we proposed that the proton of the amide moiety might be deprotonated when **1** coordinated to Zn^{2+} as shown in the Fig. 3. From the UV-vis titration data, the association constant for **1** with Zn^{2+} was determined as 3.3 (±0.1) x 10^{7} M^{-1} using Benesi-Hildebrand equation (Fig. S3).[54] This value was within the range of those (1.0 ~ 1.0 x 10^{12}) reported for Zn^{2+} sensing chemosensors.[55-58] The detection limit was estimated as 19 nM based on the 3σ/slope (Fig. S4), which was about ten thousand folds lower than the

WHO guideline (76 μM) for Zn^{2+} ions in drinking water.[35,59]

To check the practical applicability of **1** as Zn^{2+} selective sensor, fluorescence competition experiments were carried out in the presence of Zn^{2+} mixed with various metal ions. When **1** was treated with 1.5 equiv of Zn^{2+} in the presence of the same concentrations of other metal ions (Fig. 4), other background metal ions had no obvious interference with the detection of Zn^{2+} ion, except for Co^{2+} and Cu^{2+} which showed about 50 % and 70% interferences, respectively. The interferences with Co^{2+} and Cu^{2+} might be due to the strong quenching properties to fluorescence.[60,61] Nevertheless, they still showed sufficient turn-on fluorescence. In the presence of excess other metal ions (15 equiv), Hg^{2+} and Fe^{3+} interfered with some, and Co^{2+} and Cu^{2+} did completely (Fig. S5). In particular, Cd^{2+} ion which is in the same group with Zn^{2+} didn't affect the emission intensity of **1**-Zn^{2+}. These results indicated that **1** could be a good Zn^{2+} sensor which could distinguish Zn^{2+} from Cd^{2+} commonly having similar properties.

^{1}H NMR spectroscopic studies of 1 toward Zn^{2+}

The ^{1}H NMR titration experiments were studied in D_2O/CD_3OD (9:1, v/v) to further examine the binding mode between **1** and Zn^{2+} ion (Fig. 5). Upon addition of Zn^{2+} to sensor **1**, all of the aromatic and the aliphatic protons showed downfield shift. Moreover, ^{1}H NMR titration in CD_3CN showed that the proton signal of the amide moiety gradually disappeared according to the increase of Zn^{2+} (Fig. S6). These chemical shifts suggested that the oxygen atom of the ethanol moiety and the four nitrogen atoms might coordinate to Zn ion. This coordinative behavior of potentially penta-dentate ligand **1** with a zinc ion was previously observed in the similar type of zinc complexes.[36] There was no shift in the position of proton signals on further addition of Zn^{2+} (>1.5 equiv). Based on Job plot, ESI-mass spectrometry analysis, ^{1}H NMR titration, and the crystal structures of similar types of zinc complexes, we proposed the structure of **1**-Zn^{2+} complex as shown in scheme 2.

pH effect of 1 toward Zn^{2+}

To study the practical applicability of **1**, the effects of pH on the fluorescence response of Zn^{2+} were investigated at pH ranging from 2 to 12 (Fig. 6). The fluorescence intensity of **1** in the presence of Zn^{2+} showed a significant response between pH 5 and 12. These results indicated that Zn^{2+} could be clearly detected by the fluorescence spectra measurement using **1** over the environmentally and physiologically relevant pH range (pH 7.0-8.4),[62] especially for

monitoring Zn^{2+} in water samples and living cells.

Reversible test of 1 toward Zn^{2+} by using EDTA

To examine the reversibility of sensor **1** toward Zn^{2+} in buffer solution, ethylenediaminetetraacetic acid (EDTA, 1.5 equiv) was added to the complexed solution of sensor **1** and Zn^{2+}. As shown in Fig. S7, a fluorescence signal at 521 nm was immediately quenched. Upon addition of Zn^{2+} again, the fluorescence was recovered. The fluorescence emission changes were almost reversible even after several cycles with the sequentially alternative addition of Zn^{2+} and EDTA. These results indicated that sensor **1** could be recyclable simply through treatment with a proper reagent such as EDTA. Such reversibility and regeneration could be important for the fabrication of chemosensor to sense Zn^{2+}.

Biological application for Zn^{2+}

To further demonstrate the potential of **1** to monitor Zn^{2+} in living matrices, fluorescence imaging experiments were carried out in living cells (Fig. 7a). Adult human dermal fibroblasts were first incubated with various concentrations of aqueous Zn^{2+} solutions (0, 5, 10, 40, 80 and 100 μM) for 4 h and then exposed to **1** for 1 h before imaging. The experimental results showed that the fibroblast cells without either Zn^{2+} or **1** showed negligible intracellular fluorescence, while those cultured with both Zn^{2+} and **1** exhibited fluorescence. With an increase in Zn^{2+} concentration from 5 to 100 μM, the relative fluorescence intensity of the cells with **1** increased (Fig. 7b). These observations confirmed that **1** could be cell membrane permeable and thus successfully applied for the determination of Zn^{2+} in living cells.

Determination of zinc ion in water samples

In order to examine the practical properties of the chemosensor **1** in environmental samples, the chemosensor **1** was applied for the determination of Zn^{2+} in water samples, using a calibration curve of **1** toward Zn^{2+} (Fig. S8). Tap water and artificial polluted water samples were chosen. As shown in Table 1, a suitable recovery and R.S.D. values of the water samples were obtained.

Theoretical calculations

To obtain a deeper insight into the interaction of **1** with Zn^{2+}, theoretical calculations were

carried out in parallel to the experimental studies. We performed all theoretical calculations by a 1:1 stoichiometry, based on Job plot and ESI-mass analysis. As the proton of the amide group in **1** was deprotonated by Zn^{2+}, we calculated the deprotonated product for **1**-Zn^{2+} complex. Energy-minimized structures (S_0) for **1** and **1**-Zn^{2+} complex were optimized by applying density functional theory (DFT/B3LYP/6-31G**). The significant structural properties of the energy-minimized structures were indicated in Fig S9. Based on the molecular orbitals (MOs) for the ground state of **1** and **1**-Zn^{2+} complex (Fig. 8 and S10), the chelation of Zn^{2+} with **1** rendered the HOMO to LUMO energy gap of **1** decrease, which is consistent with the red shift in the UV-vis spectrum of **1**-Zn^{2+} complex. Thus, the fluorescence enhancement of **1**-Zn^{2+} complex could be explained by CHEF effect.[63,64]

Conclusion

We have developed a new ethyl alcohol-functionalized chemosensor **1**, which detected Zn^{2+} ion in aqueous solution. **1** showed highly selective fluorescence response to Zn^{2+} with the detection limit at the nanomolar level (19 nM). Importantly, **1** can clearly distinguish Zn^{2+} from Cd^{2+}, where such distinction of Zn^{2+} from Cd^{2+} is a well-known challenge. The binding of the sensor **1** and Zn^{2+} was chemically reversible with EDTA. In addition, **1** could be successfully applied to real samples with the satisfactory recovery and R.S.D. values. The living cell experiments demonstrated its value in the practical application. Moreover, the sensing mechanism of Zn^{2+} by **1** via CHEF effect was be explained by DFT calculations. Therefore, we believe that sensor **1** will be an excellent prototype for the feasible system for monitoring Zn^{2+} concentrations in biological and environmental environments.

Acknowledgements

Financial support from Basic Science Research Program through the National Research Foundation of Korea (NRF) funded by the Ministry of Education, Science and Technology (NRF-2014R1A2A1A11051794, 2012001725 and 2012008875) are gratefully acknowledged. We thank Nano-Inorganic Laboratory, Department of Nano & Bio Chemistry, Kookmin University to access the Gaussian 03 program packages.

Appendix A. Supplementary data

Supplementary data related to this article can be found at http://????.

References

[1] R. K. Pathak, V. K. Hinge, A. Rai, D. Panda and C. P. Rao, *Inorg. Chem.*, 2012, **51**, 4994–5005.

[2] A. Ajayaghosh, P. Carol and S. Sreejith, *J. Am. Chem. Soc.*, 2005, **127** 14962-14963.

[3] Y. Wu, X. Peng, B. Guo, J. Fan, Z. Zhang, J. Wang, A. Cui and Y. Gao, *Org. Biomol. Chem*., 2005, **3**, 1387-1392.

[4] P. Jiang, L. Chen, J. Lin, Q. Liu, J. Ding, X. Gao and Z. Guo, *Chem. Commun.*, 2002, 1424-1425.

[5]A. Loas, R. J. Radford and S. J. Lippard, *Inorg. Chem.*, 2014, **53**, 6491-6493.

[6] K. Tayade, B. Bondhopadhyay, H. Sharma, A. Basu, V. Gite, S. Attarde, N. Singh and A. Kuwar, *Photochem. Photobiol. Sci.*, 2014, **13**, 1052-1057.

[7] J. H. Weiss, S. L. Sensi and J. Y. Koh, *Trends Pharmacol. Sci.*, 2000, **21**, 395-401.

[8] B. K. Bitanihirwe and M. G. Cunningham, *Synapse*, 2009, **63**, 1029-1049.

[9] X. Xie and T. G. Smart, *Nature*, 1991, **349**, 521-524.

[10] C. E. Outten and T. V. O'Halloran, *Science*, 2001, **292**, 2488.

[11] Z. Xu, G.-H. Kim, S. J. Han, M. J. Jou, C. Lee, I. Shin and J. Yoon, *Tetrahedron*, 2009, **65**, 2307–2312.

[12] K. Li and A. Tong, *Sens. Actuators B*, 2013, **184**, 248–253.

[13] H. J. Kim, S. Y. Park, S. Yoon and J. S. Kim, *Tetrahedron*, 2008, **64**, 1294–1300.

[14] M. Shellaiah, Y.-H. Wu and H.-C. Lin, *Analyst*, 2013, **138**, 2931–2942.

[15] C. Gao, X. Jin, X. Yan, P. An, Y. Zhang, L. Liu, H. Tian, W. Liu, X. Yao and Y. Tang, *Sens. Actuators B*, 2013, **176**, 775–781.

[16] Y. J. Na, I. H. Hwang, H. Y. Jo, S. A. Lee, G. J. Park and C. Kim, *Inorg. Chem. Commun.*, 2013, **35**, 342-345.

[17] S. Cui, G. Liu, S. Pu and B. Chen, *Dyes Pigm.*, 2013, **99**, 950-956.

[18] Y. Li, Q. Zhao, H. Yang, S. Liu, X. Liu, Y. Zhang, T. Hu, J. Chen, Z. Chang and X. Bu, *Analyst*, 2013, **138**, 5486-5494.

[19] M. Yan, T. Li and Z. Yang, *Inorg. Chem. Commun.*, 2011, **14**, 463-465.

[20] H. Kim, J. Kang, K. B. Kim, E. J. Song and C. Kim, *Spectrochim. Acta Part A*, 2014, **118**, 883-887.

[21] V. Bhalla, H. Arora, A. Dhir and M. Kumar, *Chem. Comm.*, 2012, **48**, 4722-4724.

[22] Z. Liu, C. Zhang, Y. Chen, W. He and Z. Guo, *Chem. Commun.*, 2012, **48**, 8365-8367.

[23] K. Tayade, S. K. Sahoo, B. Bondhopadhyay, V. K. Bhardwaj, N. Singh, A. Basu, R. Bendre and A. Kuwar, *Biosens. Bioelectron.*, 2014, **61**, 429-433.

[24] V. K. Gupta, N. Mergu and A. K. Singh, *Sens. Actuators B*, 2014, **202**, 674-682.

[25] A. R. Khorrami, A. R. Fakhari, M. Shamsipur and H. Naeimi, *Environ. Anal. Chem.*, 2009, **89**, 319-329.

[26] M. Ghaedi, F. Ahmadi and A. Shokrollahi, *J. Hazard. Mater.*, 2007, **142**, 272-278.

[27] K. S. Rao, T. Balaji, T. P. Rao, Y. Babu and G. R. K. Naidu, *Spectrochim. Acta Part B*, 2002, **57**, 1333-1338.

[28] R. Gulaboski, V. Mirčeski and F. Scholz, *Electrochem. Commun.*, 2002, **4**, 277-283.

[29] G. J. Park, Y. J. Na, H. Y. Jo, S. A. Lee, A. R. Kim, I. Noh and C. Kim, *New J. Chem.*, 2014, **38**, 2587-2594.

[30] V. Bhalla, R. Kumar and M. Kumar, *Dalton Trans.*, 2013, **42**, 975–980.

[31] Y. Ma, F. Wang, S. Kambam and X. Chen, *Sens. Actuators B*, 2013, **188**, 1116–1122.

[32] K. M. K. Swamy, M. J. Kim, H. R. Jeon, J. Y. Jung and J. Yoon, *Bull. Korean Chem. Soc.*, 2010, **31**, 3611-3616

[33] Z. Xu, J. Yoon and D. R. Spring, *Chem. Soc. Rev.*, 2010, **39**, 1996-2006.

[34] E. J. Song, J. Kang, G. R. You, G. J. Park, Y. Kim, S. Kim, C. Kim and R. G. Harrison, *Dalton Trans.*, 2013, **42**, 15514-15520.

[35] H. G. Lee, J. H. Lee, S. P. Jang, H. M. Park, S. Kim, Y. Kim, C. Kim and R. G. Harrison, *Tetrahedron*, 2011, **67**, 8073-8078.

[36] H. G. Lee, J. H. Lee, S. P. Jang, I. H. Hwang, S. Kim, Y. Kim, C. Kim and R. G. Harrison, *Inorg. Chim. Acta*, 2013, **394**, 542-551.

[37] E. J. Song, G. J. Park, J. J. Lee, S. Lee, I. Noh, Y. Kim, S. -J. Kim, C. Kim and R. G. Harrison, *Sens. Actuators B*, 2015, **213**, 268-275.

[38] H. Kim, G. R. You, G. J. Park, J. Y. Choi, I. Noh, Y. Kim, S. -J. Kim, C. Kim and R. G. Harrison, *Dyes Pigm.*, 2015, **113**, 723-729.

[39] S. Sinha, T. Mukherjee, J. Mathew, S. K. Mukhopadhyay and S. Ghosh, *Anal. Chim. Acta*, 2014, **822**, 60-68. K. Hanaoka, Y. Muramatsu, Y. Urano, T. Terai and T. Nagano, *Chem. Eur. J.*, 2010, **16**, 568-572.

[40] D. Xang, X. Xiang, X. Yang, X. Wang, Y. Guo, W. Liu and W. Qin, *Sens. Actuators B*, 2014, **201**, 246-254.

[41] L. Zang, H. Shang, D. Wei and S. Jiang, *Sens. Actuators B*, 2013, **185**, 389-397.

[42] O. Akio, M. Yasuko, S. Kazuki and H. Itaru, *J. Am. Soc.*, 2004, **126**, 2454-2463.

[43] C. Lakshmi, Roger G. Hanshaw, Bradley D. Smith, *Tetrahedron*, 2004, **60**, 11307-11315.

[44] B. A. Wong, S. Friedle and S. J. Lippard, *Inorg. Chem.*, 2009, **48**, 7009-7011. A. J. Moro, P. J. Cywinski, S. Körsten and G. J. Mohr, *Chem. Commun.*, 2010, **46**, 1085-1087.

[45] H. Kim, Y. Liu, D. Nam, Y. Li, S. Park, J. Yoon and M. H. Hyun, *Dyes Pigm.*, 2014, **106**, 20-24.

[46] F. Chaumont, S. Dallongeville, N. Chenouard, N. Hervé, S. Pop, T. Provoost, V. Meas-Yedid, P. Pankajakshan, T. Lecomte, Y. L. Montagner, T. Lagache, A. Dufour, J.-C. Olivo-Marin, *Nature Methods*, 2012, **9**, 690-696.

[47] M. J. Frisch, G. W. Trucks, H. B. Schlegel, G. E. Scuseria, M. A. Robb, J. R. Cheeseman, J. A. Montgomery, Jr., T. Vreven, K. N. Kudin, J. C. Burant, J. M. Millam, S. S. Iyengar, J. Tomasi, V. Barone, B. Mennucci, M. Cossi, G. Scalmani, N. Rega, G. A. Petersson, H. Nakatsuji, M. Hada, M. Ehara, K. Toyota, R. Fukuda, J. Hasegawa, M. Ishida, T. Nakajima, Y. Honda, O. Kitao, H. Nakai, M. Klene, X. Li, J. E. Knox, H. P. Hratchian, J. B. Cross, V. Bakken, C. Adamo, J. Jaramillo, R. Gomperts, R. E. Stratmann, O. Yazyev, A. J. Austin, R. Cammi, C. Pomelli, J. W. Ochterski, P. Y. Ayala, K. Morokuma, G. A. Voth, P. Salvador, J. J. Dannenberg, V. G. Zakrzewski, S. Dapprich, A. D. Daniels, M. C. Strain, O. Farkas, D. K. Malick, A. D. Rabuck, K. Raghavachari, J. B. Foresman, J. V. Ortiz, Q. Cui, A. G. Baboul, S. Clifford, J. Cioslowski, B. B. Stefanov, G. Liu, A. Liashenko, P. Piskorz, I. Komaromi, R. L. Martin, D. J. Fox, T. Keith, M. A. Al-Laham, C. Y. Peng, A. Nanayakkara, M. Challacombe, P. M. W. Gill, B. Johnson, W. Chen, M. W. Wong, C. Gonzalez, and J. A. Pople, Gaussian 03, Revision D.01, Gaussian, Inc., Wallingford CT, 2004.

[47] A. D. Becke, *J. Chem. Phys.*, 1993, **98**, 5648-5652.

[48] C. Lee, W. Yang and R. G. Parr, *Phys. Rev. B*, 1988)37, 785-789.

[49] P. C. Hariharan and J. A. Pople, *Theor. Chim. Acta*, 1973, **28**, 213-222

[50] M. M. Francl, W. J. Petro, W. J. Hehre, J. S. Binkley, M. S. Gordon, D. F. DeFrees and J. A. Pople, *J. Chem. Phys.*, 1982, **77**, 3654-3665.

[51] N. C. Lim, J. V. Schuster, M. C. Porto, M. A. Tanudra, L. Yao, H. C. Freake and C. Brückner, *Inorg. Chem.*, 2005, **44**, 2018-2030.

[52] P. Job, *Ann. Chim.*, 1928, **9**, 113-203.

[53] T. Heinze, T. Liebert, U. Heinze and K. Schwikal, *Cellulose*, 2004, **11**, 239-245.

[54] H. A. Benesi and J. H. Hildebrand, *J. Am. Chem. Soc.*, 1949, **71**, 703-2707.

[55] H. Y. Lin, P. Y. Cheng, C. F. Wan and A. T. Wu, *Analyst*, 2012, **137**, 4415-4417.

[56] J. H. Kim, I. H. Hwang, S. P. Jang, J. Kang, S. Kim, I. Noh, Y. Kim, C. Kim and R. G. Harrison, *Dalton Trans.*, 2013, **42**, 5500-5507.

[57] W. H. Hsieh, C. Wan, D. Liao and A. Wu, *Tetrahedron Lett.*, 2012, **53**, 5848-5851.

[58] Y. Zhou, Z. Li, S. Zang, Y. Zhu, H. Zhang, H. Hou and T. C. W. Mak, *Org. Lett.*, 2012, **14**, 1214-1217.

[59] Y. P. Kumar, P. King and V. S. K. R. Prasad, *Chem. Eng. J.*, 2006, **124**, 63-70.

[60] Z. Liu, Z. Yang, T. Li, B. Wang, Y. Li, D. Qin, M. Wang, M. Yan, *Dalton Trans.*, 2011, **40**, 9370-9373.

[61] R. Homan, M. Eisenberg, *Biochim. Biophys. Acta*, 1985, **812**, 485-492.

[62] R. M. Harrison, D. P. H. Laxen and S. J. Wilson, *Environ. Sci. Technol.*, 1981, **15**, 1378-1383.

[63] A. Gogoi, S. Samanta and G. Das, *Sens. Actuators B*, 2014, **202**, 788-794.

[64] J. J. Lee, G. J. Park, Y. S. Lee, S. Y. Lee, H. J. Lee, I. Noh and C. Kim, *Biosens. Bioelectron.*, 2015, **69**, 226-229.

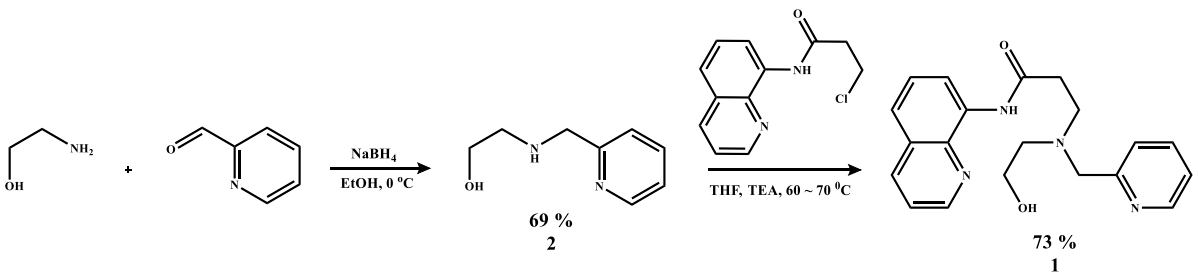

Scheme 1. Synthesis of **1**.

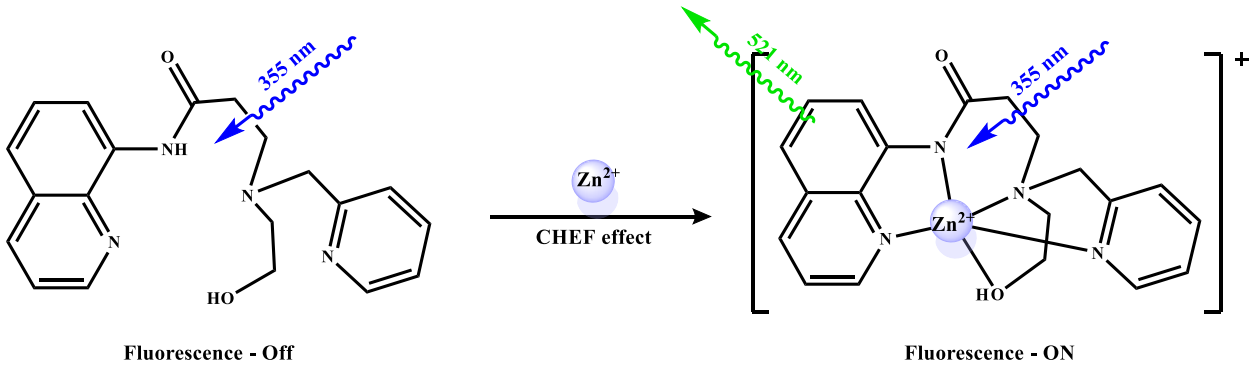

Scheme 2. Fluorescence enhancement mechanism and proposed structure of **1** in the presence of Zn^{2+}**.**

Table 1. Determination of Zn(II) in water samples

Sample	Zn(II) added (μmol/L)	Zn(II) found (μmol/L)	Recovery (%)	R.S.D. (n = 3) (%)
Tap water	0.00	0.00		
	6.00	5.9	98.5	3.1
Water sample[a]	0.00	5.8	97.3	4.2
	2.00	7.7	95.2	8.8

[a] Prepared by deionized water, 6.00 μmol/L Zn(II), 10 μmol/L Cd(II), Pb(II), Na(I), K(I), Ca(II), Mg(II). Conditions: [**1**] = 20 μmol/L in 10 mM bis-tris buffer-MeOH solution (999:1, pH 7.0).

Figure Captions

Figure 1. Fluorescence spectral changes of **1** (10 μM) in the presence of different metal ions (1.5 equiv) such as Na^{+}, K^{+}, Mg^{2+}, Ca^{2+}, Al^{3+},Ga^{3+}, Cr^{3+}, Mn^{2+}, Fe^{2+}, Fe^{3+}, Co^{2+}, Ni^{2+}, Cu^{2+}, Zn^{2+}, Ga^{3+} and Pb^{2+} with an excitation of 355 nm in buffer solution (10 mM bis-tris, pH 7.0).

Figure 2. Fluorescence spectral changes of **1** (10 μM) in the presence of different concentrations of Zn^{2+} ions in buffer solution (10 mM bis-tris, pH 7.0). Inset: Fluorescence intensity at 521 nm versus the number of equiv of Zn^{2+} added.

Figure 3. Positive-ion electrospray ionization mass spectrum of **1** (20 μM) upon addition of $Zn(NO_3)_2$ (1.5 equiv).

Figure 4. Competitive selectivity of **1** (10 μM) toward Zn^{2+} (1.5 equiv) in the presence of other metal ions (1.5 equiv) with an excitation of 355 nm in buffer solution (10 mM bis-tris, pH 7.0).

Figure 5. ^{1}H NMR titration of **1** with $Zn(NO_3)_2$ in D_2O/CD_3OD solution (D_2O/CD_3OD, 9:1, v/v).

Figure 6. Fluorescence intensity (at 521 nm) of **1** in the presence of Zn^{2+} at different pH values (2-12) in buffer solution (10 mM bis-tris, pH 7.0).

Figure 7. (a) Fluorescence images of fibroblasts cultured with Zn^{2+} and **1**. Cells were exposed to 0 (A and G), 5 (B and H), 10 (C and I), 40 (D and J), 80 (E and K) and 100 μM (F and L) $Zn(NO_3)_2$ for 4 h and then later with **1** for 1 h. The top images (A-F) were observed with the light microscope and the bottom images (G-L) were taken with a fluorescence microscope. The scale bar is 50 μm. (b) Quantification (green light source) of mean fluorescence intensity in the bottom images (G-L).

Figure 8. Molecular orbital diagrams participating in the singlet state for the **1** and **1**-Zn^{2+} complex.

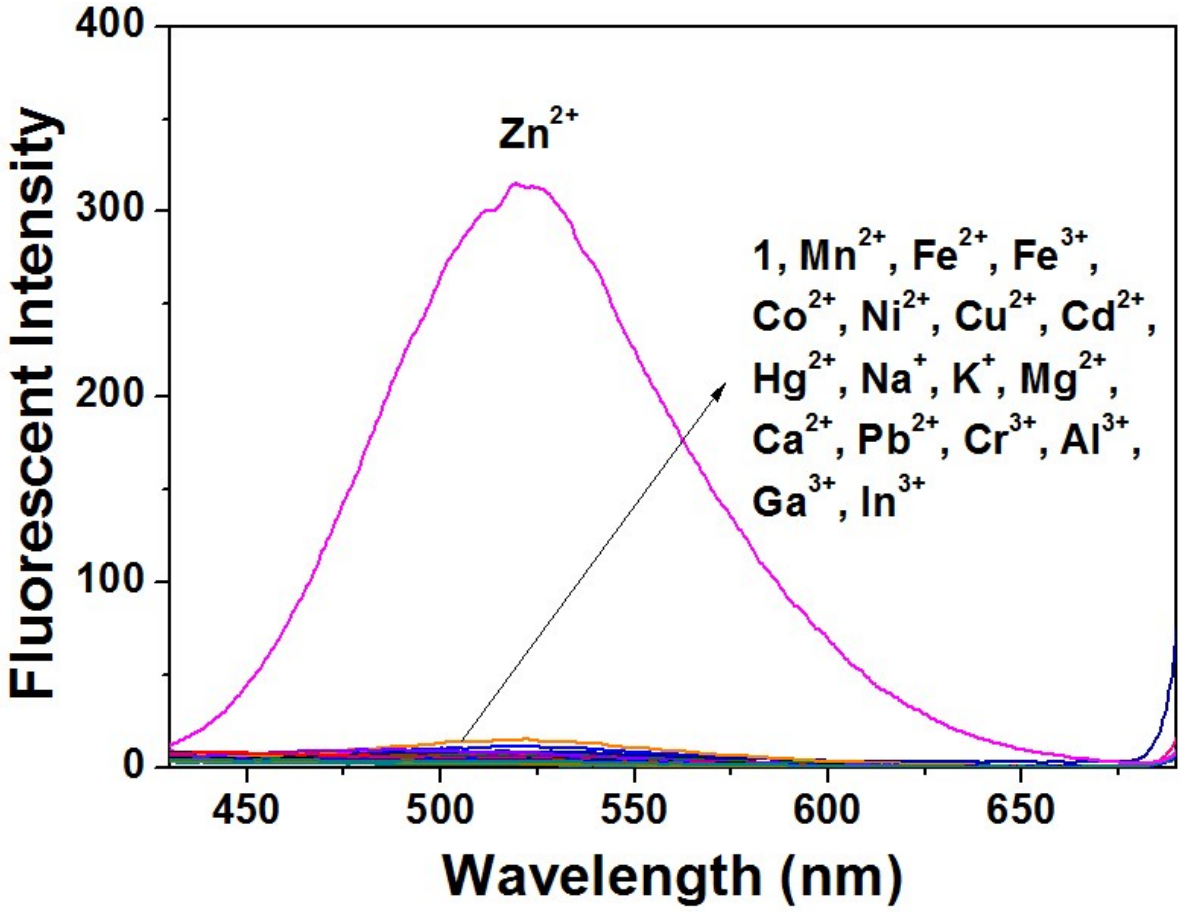

Fig. 1.

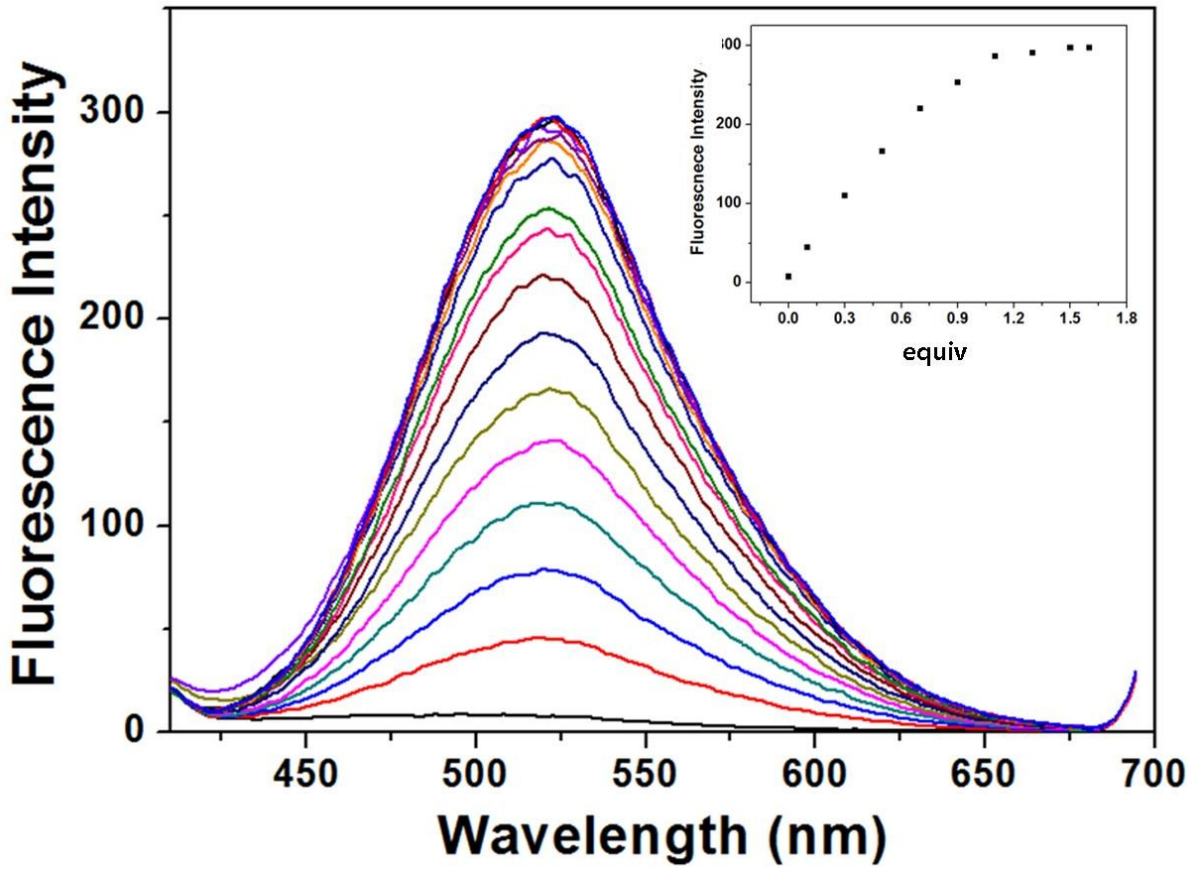

Fig. 2.

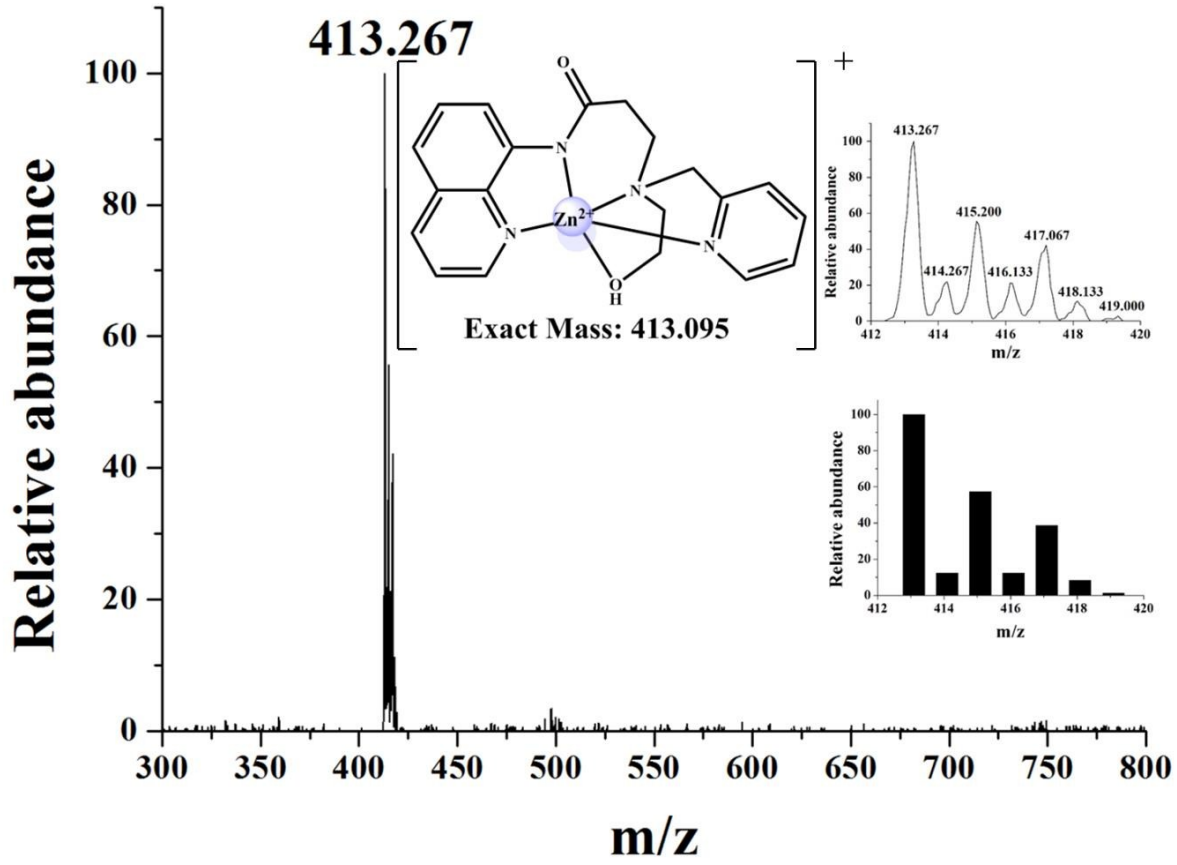

Fig. 3.

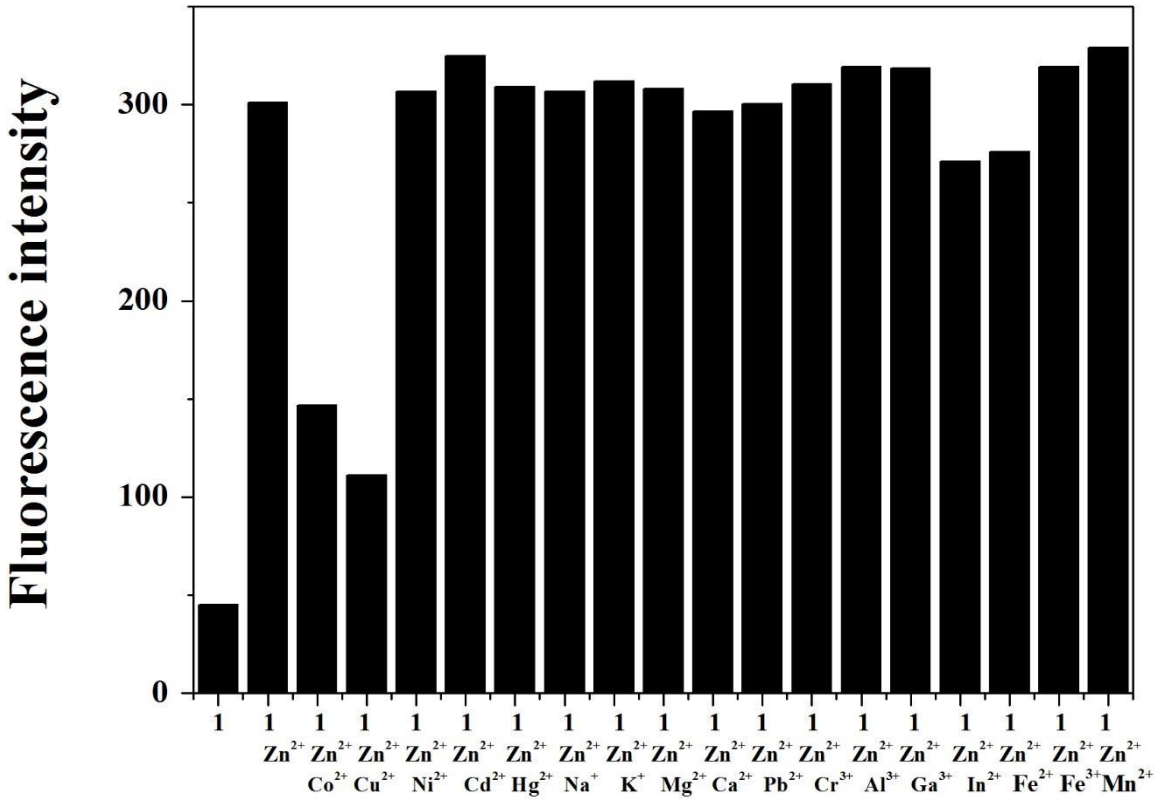

Fig. 4.

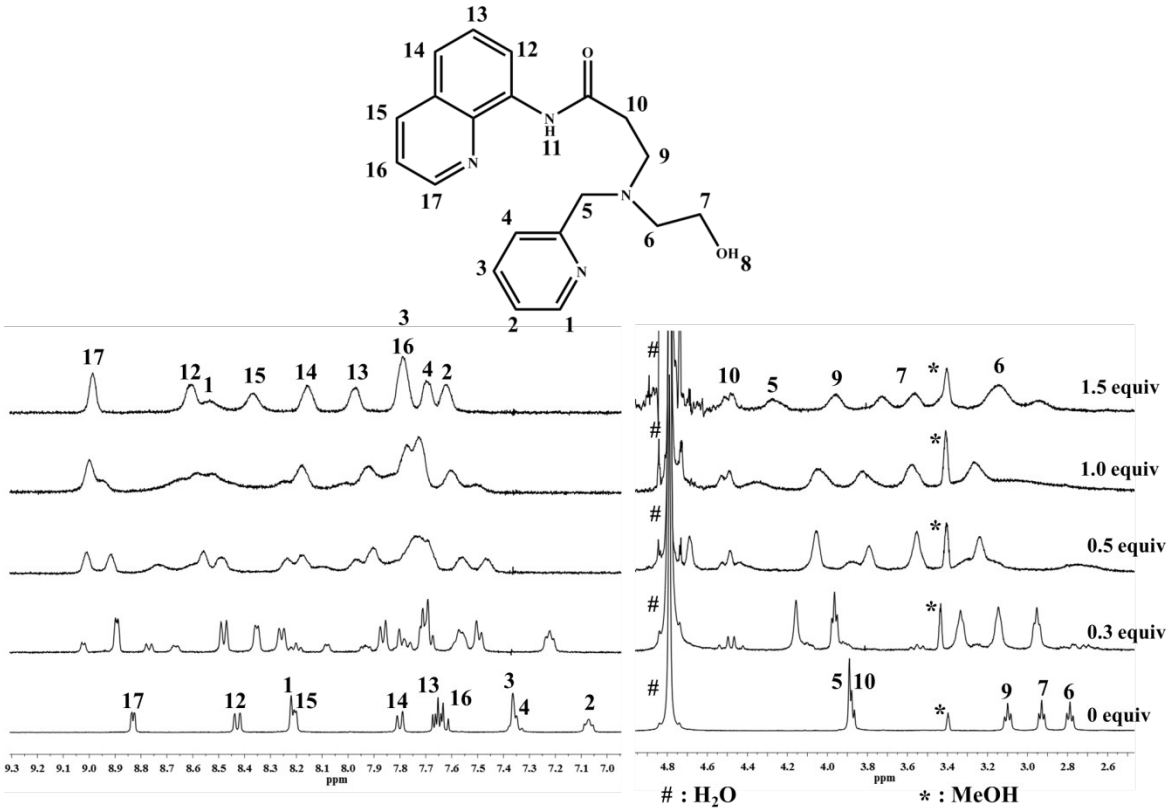

Fig. 5.

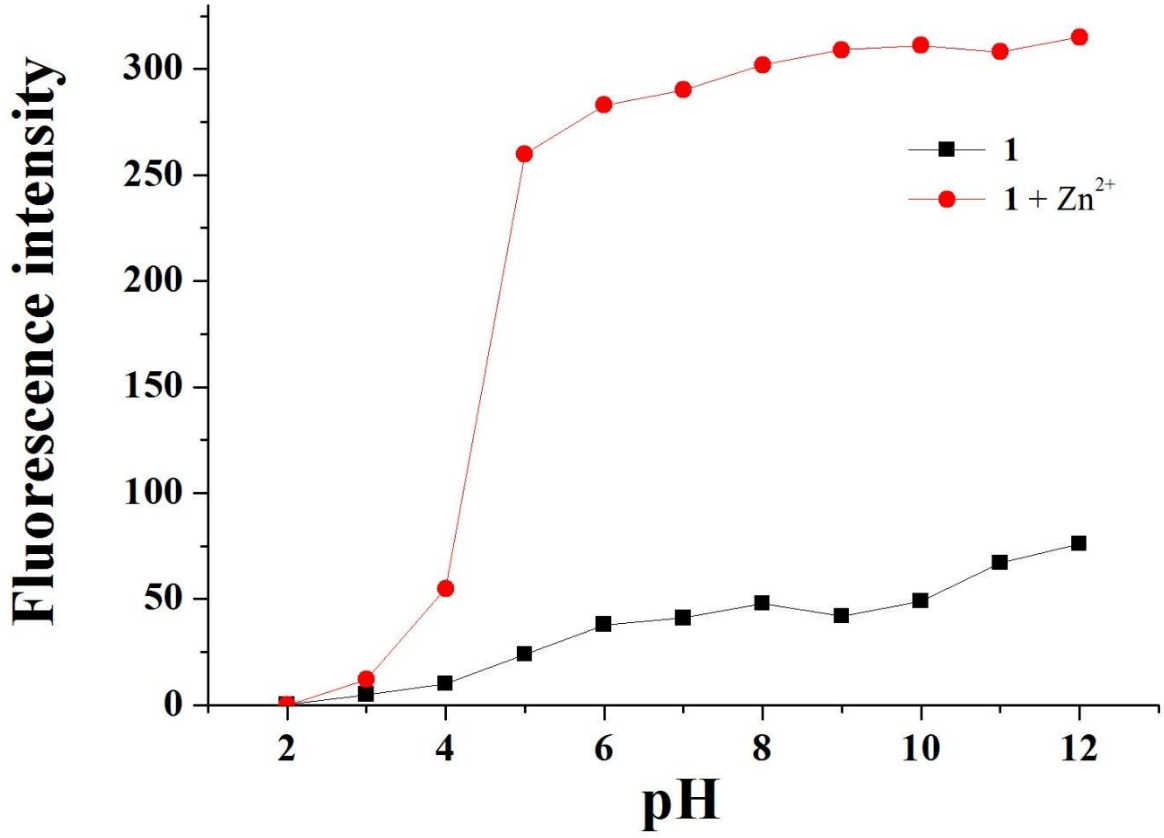

Fig. 6.

(a)

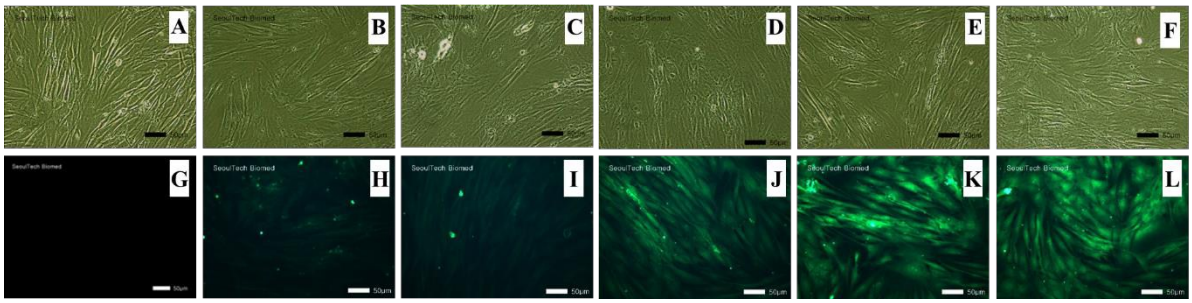

(b)

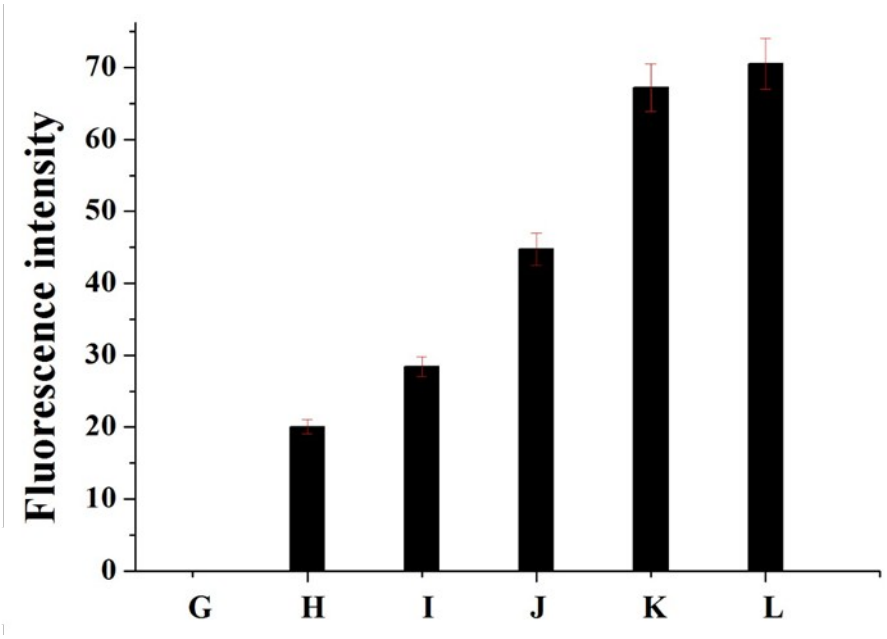

Fig. 7.

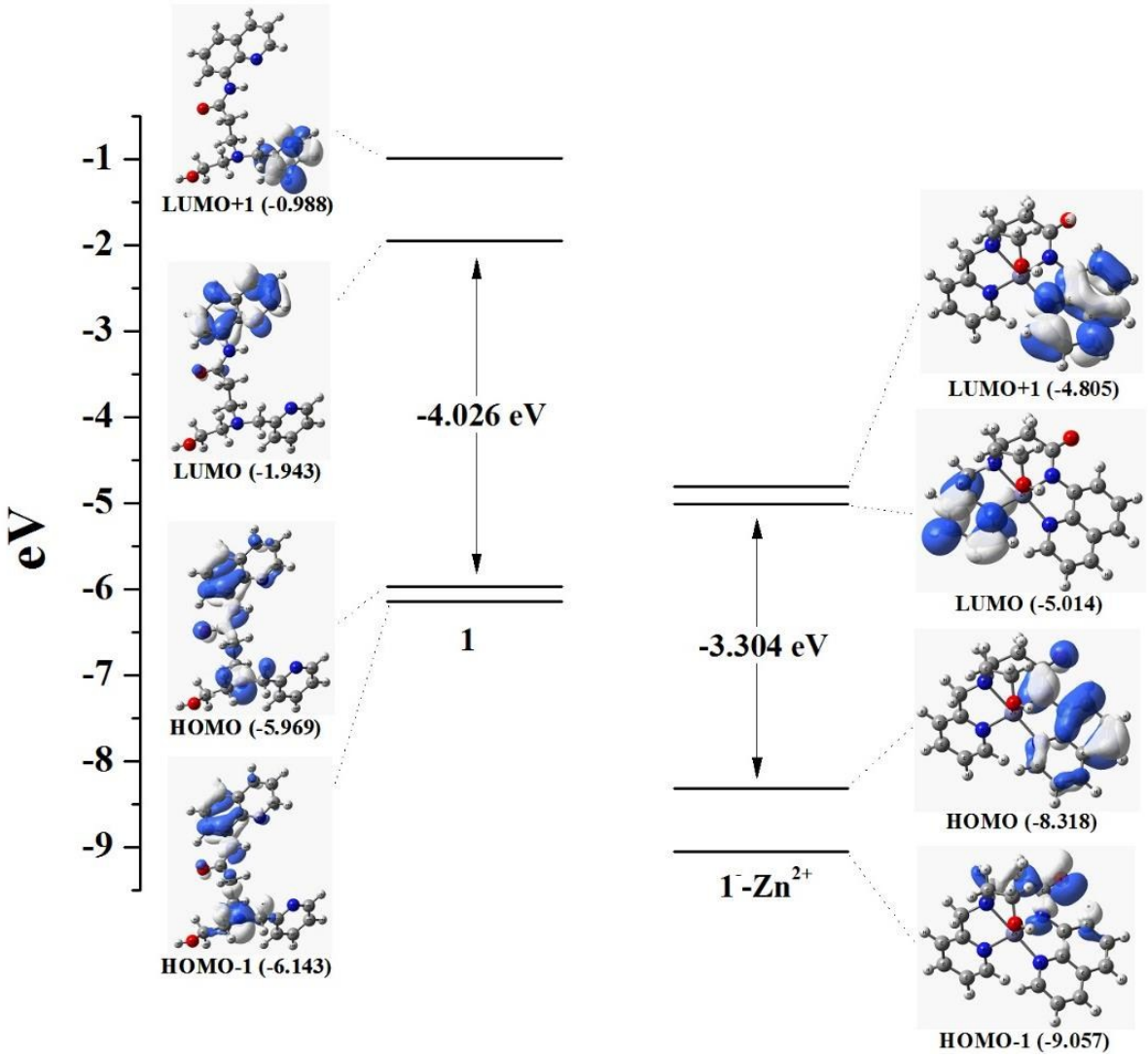

Fig. 8.